Journal of Alloys and Compounds 771 (2019) 664–673

Contents lists available at ScienceDirect

Journal of Alloys and Compounds

journal homepage: http://www.elsevier.com/locate/jalcom

# Theoretical research on structural, electronic, mechanical, lattice dynamical and thermodynamic properties of layered ternary nitrides $Ti_2AN$ (A = Si, Ge and Sn)

A. Candan [a, *], S. Akbudak [b], Ş. Uğur [c], G. Uğur [c]

[a] Department of Machinery and Metal Technology, Ahi Evran University, 40100, Kırşehir, Turkey
[b] Department of Physics, Faculty of Arts and Sciences, Adıyaman University, 02100, Adıyaman, Turkey
[c] Department of Physics, Faculty of Science, Gazi University, 06500, Ankara, Turkey

ARTICLE INFO

*Article history:*
Received 31 July 2018
Received in revised form
27 August 2018
Accepted 28 August 2018
Available online 31 August 2018

*Keywords:*
MAX phases
Electronic properties
Nitrides
Mechanical properties
Lattice dynamics
Thermodynamic properties

ABSTRACT

First-principles density functional theory (DFT) calculations within generalized gradient approximation (GGA) are carried out to investigate the structural, electronic, mechanical, lattice dynamical and thermodynamic properties of $Ti_2AN$ (A = Si, Ge and Sn) MAX phases. The optimized geometrical parameters such as lattice constants ($a$, $c$) and the internal coordinates have been calculated. Electronic band structure and corresponding density of states (DOS) have been obtained. The analysis of the band structures and density of states have shown that these compounds are electrical conductors. The elastic constants have been ascertained using the stress-strain method. The isotropic elastic moduli, known as bulk modulus ($B$), shear modulus ($G$), young's modulus ($E$), poisson's ratio ($\nu$), vickers hardness ($H_v$) and linear compressibility coefficients ($\alpha$) have been studied within framework of the Voigt–Reuss–Hill approximation for ideal polycrystalline $Ti_2AN$ (A = Si, Ge and Sn) MAX aggregates. Furthermore, the phonon dispersion curves as well as accompanying phonon density of states have been comprehensively computed. And also raman and infrared modes at the Γ point have been obtained. Within the thermodynamic properties, specific heat capacity, entropy, helmholtz free energy and internal energy changes were analyzed depending on the temperature of $Ti_2AN$ (A = Si, Ge and Sn) compounds. The obtained results are presented in comparison with present theoretical data for $Ti_2SiN$. This is the first quantitative theoretical study of the electronic properties and other properties for $Ti_2GeN$ and $Ti_2SnN$ compounds and therefore theoretical results for these compounds need to be verified experimentally.


## 1. Introduction

MAX phases have attracted great interest since their discovery in the 1960s by Nowotny and co-workers [1,2]. Fundamentally, these materials are of scientific interest because of their physical and chemical characteristics such as high melting point, high bulk modulus, well oxidation resistance, low density, high thermal and electrical conductivity, thermal diffusivity, perfect thermal shock resistance and simple machinability [3–5]. Therefore, MAX phases are promising materials for heating elements, nozzles, heat exchangers and tools for depressing [6]. MAX phase compounds have general formula of $M_{n+1}AX_n$ where M is a transition metal, A is an A-group element and X is $C$ or $N$ and $n$ varies from 1 to 3. MAX phase compounds have a wide-spectrum composition and nano-layered crystal structure. These materials can be divided into three main groups based on their stoichiometric structures. These groups are known as 211, 312 and 413 materials. Except for some stoichiometric structures belonging to 413 group, most of the MAX phases were discovered in 1960s. Additionally, these materials have both ceramic and metallic phases [7]. In ceramic phase, they exhibit maximum hardness [8], resistance to oxidation [9] and being stable at high temperatures [10]. However, they show machinability [11], thermal shock resistance [12], high thermal [13] and electrical conductivity [14,15] in metallic phase. MAX phase compounds combining the superior characteristics of ceramics and metals together are seen as a transition material class between ceramics and metals. As a result, MAX phase alloys can be used as bulk, powder, foam or coating materials in industrial applications. There

* Corresponding author.
*E-mail address:* acandan@ahievran.edu.tr (A. Candan).

https://doi.org/10.1016/j.jallcom.2018.08.286
0925-8388/

are nearly 100 MAX phases at the present time. So far, however, experimentally synthesized or theoretically estimated phases belong to 211 $M_2AX$ phases such as $Ti_2AlC$, $Ti_2AlN$, $Ti_2SiC$ and $Ti_2SiN$ [16].

Owing to their intriguing features MAX phases have been subject of many experimental and theoretical studies [16–28]. Experimentally, Farle et al. [17] published autonomous crack healing for $Ti_2AlC$ and $Ti_3AlC_2$ of the $M_{n+1}AX_n$ (MAX) phase ceramics. They found that $Ti_3SiC_2$ met the criteria for autonomous high-temperature crack healing. Tian et al. have synthesized $Cr_2AlC$, and extensively investigated its thermal and electrical properties [18]. In another study, Schneider et al. have determined the structure of $Cr_2AlC$ experimentally, and performed *ab-initio* calculations for further investigations [19]. Lately, a new ternary nanolaminated carbide $Mo_2Ga_2C$ phase has been discovered by Hu et al. [20]. First-principles study of the fundamental properties have been inclusively computed for $Ti_{n+1}GaN_n$ (n = 1, 2, and 3) and $M_2AB$ (M = Ti, Zr, Hf; A = Al, Ga, In) MAX phases Surucu et al. [21,22]. Lin et al. [23] fabricated Ta–Al–C ceramics with the help of hot-pressing method using elemental Ta, Al, and graphite powders as starting materials. The mentioned authors obtained bulk modulus of Ta–Al–C carbides using Generalized Gradient Approximation and Perdew Wang exchange functional [24] in the Cambridge Sequential Total Energy Package code. First-principles study on the structural, elastic and electronic properties of $Ti_2SiN$ under high pressure have been calculated via the local density approximation (LDA) and the generalized gradient approximation (GGA) by Li et al. [28]. They have emphasized that shear anisotropy factor as well as Poisson's ratio of $Ti_2SiN$ grow with pressure. Similarly, Gan et al. [26] were systematically studied similar properties of $Ti_2SiN$ by means of first principles density functional theory calculations. It was found that $Ti_2SiN$ compound is conductive from electronic band structure. Keast et al. [27] predicted the stability of the MAX phases from first-principles calculations and the result of a small energy suggests that $Ti_2SiN$ has the potential to be fabricated as a metastable compound.

As far as we know there is no theoretical study about $Ti_2GeN$ and $Ti_2SnN$. In the current study, we looked through the electronic, mechanical, lattice dynamical and thermodynamic properties of $Ti_2AN$ (A = Si, Ge and Sn) MAX phases by means of *ab-initio* calculations.

## 2. Calculation method

The *ab-initio* calculations in this study were conducted employing the plane-wave pseudo-potential density functional theory (DFT) approach through the Vienna Ab Initio Simulation Package (MedeA-VASP) [29,30] together with the projector augmented wave potential [31]. The electronic exchange-correlation was operated by using the generalized gradient approximation (GGA) of Perdew–Burke–Ernzerhof (PBE) [32]. The plane-wave energy cut-off was opted to be 600 eV for the computation of structural, electronic, mechanical, lattice dynamical and thermodynamic properties of $Ti_2AN$ (A = Si, Ge and Sn) MAX phases. The electronic energy convergence gauge adjusted to $10^{-5}$ eV value by employing the Normal (blocked Davidson) algorithm. The Brillouin-zone integrations were performed via the Methfessel-Paxton smearing method [33] with smearing parameter of 0.1 eV. Nevertheless, a $24 \times 24 \times 5$ Monkhorst–Pack [34] *k*-point mesh were utilized for hexagonal structure. The elastic constants were acquired by the stress-strain [35] method. The phonon dispersion spectra of the noted compounds were computed with the aid of using the direct approach [36]. The forces in this approach is provided by the Hellmann–Feynman (HF) theorem. The Hellmann–Feynman forces on all atomic positions obtained for positive and negative movements with the width of 0.02 Å. $3 \times 3 \times 1$ supercells with displaced atoms containing 72 atoms were used for lattice dynamical and thermodynamic properties.

## 3. Results and discussions

### 3.1. Structural and electronic properties

MAX phases are a group of layered ternary compounds with the general formula $M_{n+1}AX_n$. $Ti_2AN$ (A = Si, Ge and Sn) compounds crystallize in two different forms in hexagonal structure $P6_3/mmc$ (No. 194) space group symmetry, where the Ti atom is located at the Wyckoff positions 4f (1/3, 2/3, *z*), while A atom is located at the 2d (1/3, 2/3, 3/4), and N at 2a (0, 0, 0).

Crystal structure of $Ti_2AN$ (A = Si, Ge and Sn) compounds are shown Fig. 1. The lattice parameters, a, c, and the internal structural parameter z, determined from geometry optimization and are given in Table 1 along with the present theoretical results for $Ti_2AN$ (A = Si, Ge and Sn). The calculated lattice parameters are; $a = 2.992$ Å and $c = 12.779$ Å for $Ti_2SiN$, $a = 3.046$ Å and $c = 12.907$ Å for $Ti_2GeN$, $a = 3.176$ Å and $c = 13.468$ Å for $Ti_2SnN$. Our results for $Ti_2SiN$ agree well with the previous theoretical results [26–28]. The calculated lattice constants *a* and *c* for $Ti_2SiN$ diverge from Ref. 26 within 0.44% and 0.32%, respectively. It has been observed that the lattice constant *a* and free internal parameters *z* increase as one goes from $Ti_2SiN$ to $Ti_2SnN$ in accordance with soaring ionic radius of the A atom. Conversely, the second lattice parameter *c* decreases.

The calculated numeral (*N*) of total density of states at the Fermi level ($E_F$) is 2.294, 3.369 and 4.704 eV, respectively for $Ti_2SiN$, $Ti_2GeN$ and $Ti_2SnN$. This value for $Ti_2SiN$ has been found to be 3.67 eV [26] and 3.59 eV [28] in two different studies. As a consequence, there is gradually increasing tendency in the DOS at $E_F$ with rising atomic numbers of the A atom. In conclusion, $Ti_2SnN$ is more conductive than $Ti_2GeN$ and $Ti_2GeN$ is more conductive than $Ti_2SiN$.

The band structures of $Ti_2AN$ (A = Si, Ge and Sn) compounds have been estimated along the high-symmetry lines within the first Brillouin zone from the computed stability lattice constant. The

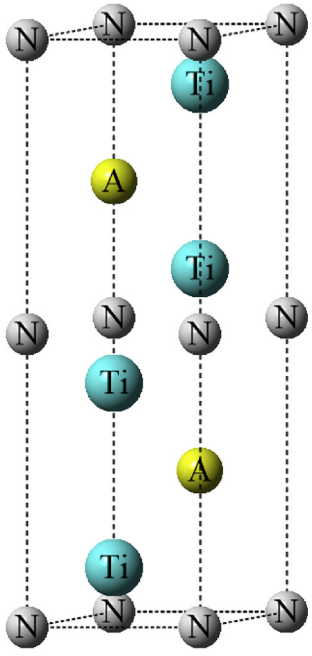


**Fig. 1.** Crystal structure of $Ti_2AN$ (A = Si, Ge and Sn) compounds.

**Table 1**
Calculated lattice parameters and Wyckoff position of $Ti_2AN$ (A = Si, Ge and Sn).

| Compounds | References | *a* (Å) | *c* | *c/a* | $Z_{Ti}$ |
|---|---|---|---|---|---|
| $Ti_2SiN$ | Present | 2.992 | 12.779 | 4.27 | (1/3,2/3,0.093) |
| | [26] | 2.979 | 12.82 | 4.30 | (1/3,2/3,0.093) |
| | [27] | 2.990 | 12.88 | 4.31 | (1/3,2/3,0.092) |
| | [28-LDA] | 2.927 | 12.617 | 4.31 | – |
| | [28-GGA] | 2.984 | 12.822 | 4.30 | – |
| $Ti_2GeN$ | Present | 3.046 | 12.907 | 4.24 | (1/3,2/3,0.089) |
| $Ti_2SnN$ | Present | 3.176 | 13.468 | 4.24 | (1/3,2/3,0.078) |

calculated band structures and relevant partial and total electronic density of states (DOS) for $Ti_2AN$ (A = Si, Ge and Sn) are shown in Fig. 2 and Fig. 3, successively. From the electronic band structure shown in Fig. 2 we can see that a) $Ti_2SiN$, b) $Ti_2GeN$ and c) $Ti_2SnN$ compounds are metallic due to the fact that there is no band gap along the Fermi level ($E_F$). The valence and conduction bands overlap greatly and there are many bands across $E_F$, which is similar to those in many $M_{n+1}AX_n$ phases [22]. As a result $Ti_2AN$ (A = Si, Ge and Sn) are expected to exhibit metallic, thermal and electrical

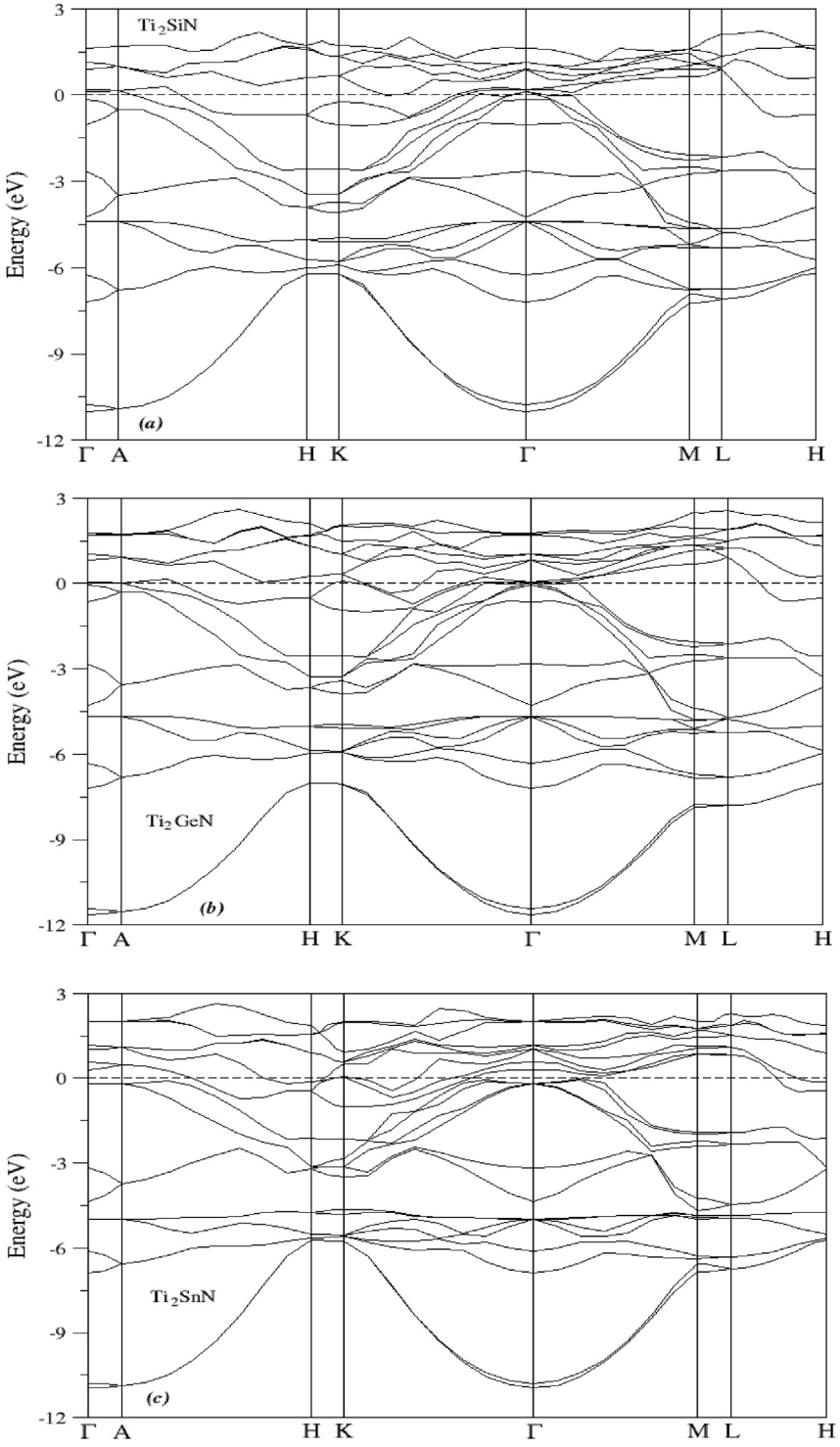


**Fig. 2.** The electronic band structure for (a) $Ti_2SiN$, (b) $Ti_2GeN$ and (c) $Ti_2SnN$ compounds.

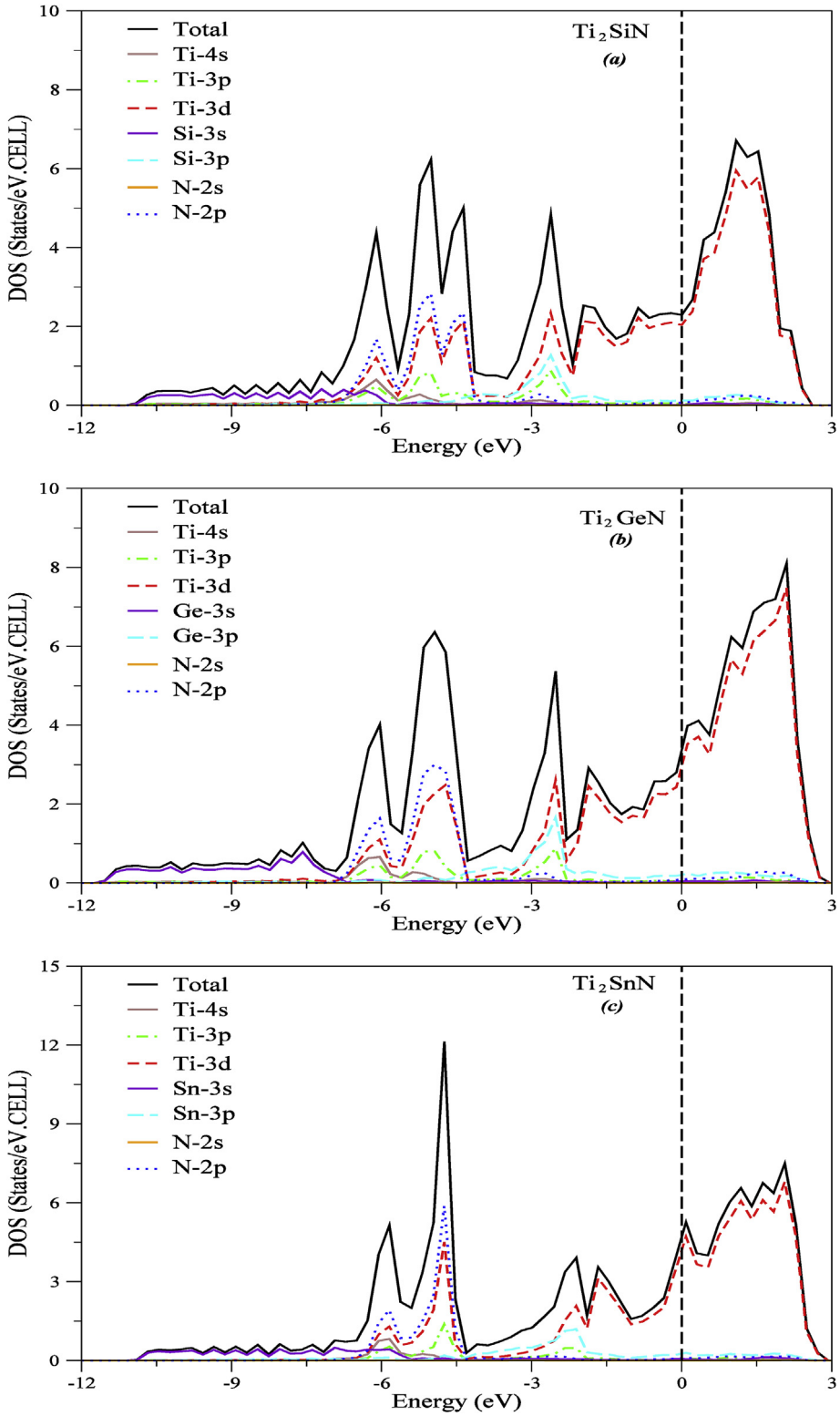


**Fig. 3.** The total and partial DOS of (a) $Ti_2SiN$, (b) $Ti_2GeN$ and (c) $Ti_2SnN$ compounds.

conduction. The calculated partial and total density of states (DOS) of a) $Ti_2SiN$, b) $Ti_2GeN$ and c) $Ti_2SnN$ compounds are shown in Fig. 3. DOS is the most important electronic property in materials science and condensed matter physics and it is defined as the number of allowed electron (or hole) states per volume at a given energy [37,38]. It is clear that all alloys are metallic due to the fact that the DOS values differ from zero at the Fermi level. From Fig. 3 (a) it is clearly seen that for $Ti_2SiN$, between −10 eV and −7.5 eV the most contribution to DOS comes from 3s orbitals of Si atom (Si-3s). However, the least contribution comes from 3p orbitals of Si atom

(Si-3p), 3d orbitals of Ti atom (Ti-3d), 3p orbitals of Ti atom (Ti-3p) and 2p orbitals of N atom (N-2p). This is due to fact that 3p orbitals of Si atom, 3d orbitals of Ti atom, 3p orbitals of Ti atom and 2p orbitals of N atom have almost equal contribution to DOS. At −6 eV energy, the most contribution to DOS comes from 2p orbitals of N atom (N-2p) while the minor contribution comes from 3p orbitals of Si atom (Si-3p). At −3 eV the majority of the contribution to DOS comes from the 3d orbitals of Ti atom (Ti-3d) atom, while the minority of the contribution comes from 3s orbitals of Si atom (Si-3s). Between −1.5 eV and +1.5 eV the most contribution to DOS comes from the 3d orbitals of Ti atom and the least contribution to DOS comes from the 2p orbitals of N atom (N-2p) and 3s orbitals of the Si atom (Si-3s). Our calculated total and PDOS for $Ti_2SiN$ agree well with the available theoretical results [26,27].

For $Ti_2GeN$ shown in Fig. 3 (b), between −10.5 eV and −7.5 eV the majority of the contribution to DOS comes from the 3s orbitals of the Ge atom. Between −6 eV and −7.5 eV, the majority of the contribution to DOS comes from the 3p orbitals of Ti atom, 3d orbitals of Ti atom, 4s orbitals of Ti atom and 2p orbitals of N atom. At −3 eV, the majority of the contribution to DOS comes from the 3d orbitals of Ti atom, 3p orbitals of Ti atom and 3p orbitals of Ge atom. Fermi level generally consist of 3d orbitals of Ti atom. For instance, the contribution of one peak, above the Fermi level (nearly 2 eV), is mainly dominated by Ti-3d states.

For $Ti_2SnN$ case shown in Fig. 3 (c), between −10.5 eV and −7.5 eV, the majority of the contribution to DOS comes form the 3s orbitals of the Sn atom (Sn-3s). On the other hand, the minority of the contribution to DOS comes from the 3p orbitals of the Sn atom (Sn-3p). At −6 eV energy, the most contribution to DOS comes from 2p orbitals of N atom (N-2p) and 3d orbitals of the Ti atom (Ti-3d). Likewise, between −6 eV and −4,5 eV, the major contribution to DOS comes from the 2p orbitals of the N atom (N-2p), 3d orbitals of the Ti atom (Ti-3d) and the minor contribution comes from the 3p orbitals of the Sn atom (Sn-3p). From −1,5 eV until +3 eV, the most contribution to DOS comes from 3d orbitals of the Ti atom (Ti-3d) while the least contribution to DOS comes from the 2p orbitals of the N atom (N-2p) and 3s orbitals of the Sn atom (Sn-3s).

### 3.2. Mechanical properties

The elastic constant of a crystal is defined as a measure of the response of the crystal to an external stress applied to the elasticity. Therefore, the information obtained from the accurate calculation of the elastic constants plays a very important role when it is desired to examine the hardness of the material, the mechanical stability and the bond strengths between the nearest neighbor atoms of the constituent atoms. In this study, the mechanical properties of $Ti_2AN$ (A = Si, Ge and Sn) compounds are achieved by the stress-strain method. For a compound in the hexagonal structure, there are six independent elastic constants, (i.e. $C_{11}$, $C_{12}$, $C_{13}$, $C_{33}$, $C_{44}$ and $C_{66}$). Elastic constants of $Ti_2AN$ (A = Si, Ge and Sn) compounds calculated at zero temperature and zero pressure are given in Table 2 together with other theoretical studies. For mechanical stability of a crystal in hexagonal structure, the second order elastic constants must satisfy the following Born stability criteria [39],

$$C_{11} > |C_{12}|, C_{44} > 0, (C_{11} + 2C_{12})C_{33} > 2C_{13}^2 \quad (1)$$

Given these stability considerations, it is understood from Table 2 that these compounds are mechanically stable. Calculated values of $C_{13}$, $C_{33}$ and $C_{44}$ are quite concordance with previous theoretical calculations [26, 28-GGA]. The obtained $C_{12}$ value for $Ti_2SiN$ is bigger than formerly reported, but $C_{11}$ is smaller. Since there is no data that can be compared with calculated elastic constants for $Ti_2GeN$ and $Ti_2SnN$ compounds, these values are a reference for future investigations. Additionally, mechanical properties such as bulk modulus ($B$), shear modulus ($G$), young modulus ($E$), poisson's ratio ($\nu$), vickers hardness ($H_v$) and linear compressibility coefficients ($\alpha$) are calculated employing the Voigt-Reuss-Hill approximation and results are reported in Table 3 [40–42]. It has been observed that the available results are close to those of theoretical results [26, 28-GGA]. Bulk modulus ($B$), shear modulus ($G$) and young modulus ($E$) have been computed by using the equations noted below.

$$B = \frac{B_V + B_R}{2} \quad (2)$$

$$G = \frac{G_V + G_R}{2} \quad (3)$$

$$E = \frac{9BG}{(3B + G)} \quad (4)$$

**Table 2**
Calculated elastic constants $C_{ij}$ (in GPa) for $Ti_2AN$ (A = Si, Ge and Sn).

| Compounds | References | $C_{11}$ (GPa) | $C_{12}$ (GPa) | $C_{13}$ (GPa) | $C_{33}$ (GPa) | $C_{44}$ (GPa) |
|---|---|---|---|---|---|---|
| $Ti_2SiN$ | Present | 280.40 | 110.72 | 128.94 | 347.22 | 155.36 |
| | [26] | 298 | 96 | 127 | 347 | 153 |
| | [28-LDA] | 342.1 | 106.7 | 149.5 | 409.9 | 181.3 |
| | [28-GGA] | 296.7 | 100.2 | 126.3 | 347.8 | 155.1 |
| $Ti_2GeN$ | Present | 230.13 | 117.87 | 124.34 | 283.46 | 119.73 |
| $Ti_2SnN$ | Present | 220.29 | 85.3 | 80.93 | 251.45 | 78.31 |

**Table 3**
Calculated bulk modulus $B$ (in GPa), shear modulus $G$ (in GPa), young modulus $E$ (in GPa), machinability index $\mu_D$, machinability index $\mu_M$, poisson's ratio $\nu$, shear anisotropic factor $A$, hardness $H_v$ (in GPa) and linear compressibility coefficients $\alpha$ for $Ti_2AN$ (A = Si, Ge and Sn).

| Compounds | References | $B$ (GPa) | $G$ (GPa) | $E$ (GPa) | $\mu_D$ | $\mu_M$ | $\nu$ | $A$ | $H_V$ (GPa) | $\alpha$ |
|---|---|---|---|---|---|---|---|---|---|---|
| $Ti_2SiN$ | Present | 181.39 | 110.57 | 275.69 | 1.64 | 1.17 | 0.247 | 1.68 | 14.58 | 0.61 |
| | [26] | 182 | 118 | 291 | 1.54 | 1.36 | 0.233 | 1.57 | 16.63 | 0.63 |
| | [28-LDA] | 209.7 | 138.3 | 340.1 | 1.52 | 1.16 | 0.230 | 1.601 | 18.97 | 0.58 |
| | [28-GGA] | 181.9 | 117.8 | 290.7 | 1.54 | 1.17 | 0.234 | 1.583 | 16.58 | 0.65 |
| $Ti_2GeN$ | Present | 163.14 | 79.52 | 205.21 | 2.05 | 1.36 | 0.290 | 1.81 | 8.16 | 0.62 |
| $Ti_2SnN$ | Present | 131.65 | 74.24 | 187.47 | 1.77 | 1.68 | 0.263 | 1.01 | 9.71 | 0.84 |

In these equations, the subscripts $V$ and $R$ represent Voigt and Reuss's boundary values, respectively. Bulk modulus ($B$) is defined as a measure of the energy required to produce a deformation. The bulk modulus of $Ti_2SiN$, $Ti_2GeN$ and $Ti_2SnN$ compounds are found to be 181.39 GPa, 163.14 GPa, and 131.65 GPa, respectively. When bulk modulus of these alloys are compared, it is observed that there is a following correlation; $Ti_2SiN > Ti_2GeN > Ti_2SnN$. In other words, bulk modulus of $Ti_2AN$ compounds decrease as A atom goes from Si to Sn, which is plainly seen from Table 3. $G$ is known as a material resistance to shape change. Similarly, the shear modulus ($G$) demonstrates the above sequence for $Ti_2AN$ (A = Si, Ge and Sn) compounds. The young's modulus ($E$) is an important measure of hardness, and the larger the $E$ value, the harder the material is. When the shear and young modulus of $Ti_2SiN$ compound are compared, it is seen that both $E$ and $G$ are smaller than those of previous results. Hardness ordering of materials according to young modulus value for $Ti_2AN$ (A = Si, Ge and Sn) is given as $E$ ($Ti_2SiN$) > $E$ ($Ti_2GeN$) > $E$ ($Ti_2SnN$).

Ductility ($\mu_D$) and machinability ($\mu_M$) index for $Ti_2AN$ (A = Si, Ge and Sn) compounds are given in Table 3 together with the present results. The ratio of $\mu_D = B/G$ proposed by Pugh [43] is accepted as a measure of ductility or brittleness of a material. If $\mu_D$ is smaller than 1.75, the material behaves in nature a brittle manner; or else, the material behaves a ductile manner. It is openly seen from Table 3 that $Ti_2SiN$ is brittle whereas $Ti_2GeN$ and $Ti_2SnN$ are ductile. Machinability index ($\mu_M$) was presented by Sun et al. [44], which is defined as $\mu_M = B/C_{44}$. As can be seen from Table 3, the material with the biggest machinability index is $Ti_2SnN$ ($\mu_M = 1.68$). On the other hand, the value of the machinability index is found to be 1.17, 1.36 for $Ti_2SiN$ and $Ti_2GeN$, respectively.

Besides, poisson's ratio ($\nu$), shear anisotropic factor ($A$), hardness ($H_v$) and linear compressibility coefficients ($\alpha$) are computed with the equations noted below and listed in Table 3.

$$\nu = \frac{1}{2}\left[\frac{B - \frac{2}{3}G}{B + \frac{1}{3}G}\right] \tag{5}$$

$$A = \frac{4C_{44}}{(C_{11} + C_{33} - 2C_{13})} \tag{6}$$

$$H_V = 2\left(k^2G\right)^{0.585} - 3; (k = G/B) \tag{7}$$

$$\alpha = \frac{k_c}{k_a} = \frac{C_{11} + C_{12} - 2C_{13}}{C_{33} - C_{13}} \tag{8}$$

The poisson's ratio ($\nu$) is an indication of the degree of covalent bonding. The value of $\nu$ is close to 0.1 for covalent materials and 0.25 for ionic materials. The calculated poisson's ratios of $Ti_2SiN$, $Ti_2GeN$ and $Ti_2SnN$ compounds are 0.247, 0.290 and 0.263, successively as seen in Table 3. As the poisson's ratio values are around 0.25, it can be said that the ionic character is predominant in all compounds.

The shear anisotropic factor ($A$) may give information as regards isotropic or anisotropic property of a solid and for a hexagonal crystal. If the material is elastically isotropic, the value of the anisotropy factor is 1, otherwise it is different from 1 and the material is anisotropic. In this study, the calculated shear anisotropic factors for $Ti_2SiN$, $Ti_2GeN$ and $Ti_2SnN$ compounds are found to be 1.68, 1.81 and 1.01, successively as given in Table 3. For this reason, $Ti_2SiN$ and $Ti_2GeN$ compounds is elastically anisotropic while $Ti_2SnN$ compound has isotropic characteristic.

The another significant mechanical feature of a crystalline solid is vickers hardness ($Hv$) that may be calculated from a semi-empirical technique [45] as seen in Eq. (7). As seen in Table 3, $Ti_2SiN$ has the highest hardness (14.58 GPa), whereas $Ti_2GeN$ has the smallest hardness (8.16 GPa).

Finally, the linear compressibility coefficients of $Ti_2AN$ (A = Si, Ge and Sn) compounds in hexagonal structure are calculated from Eq. (8). The estimated linear compressibility coefficients for $Ti_2SiN$, $Ti_2GeN$ and $Ti_2SnN$ compounds are 0.61, 0.62 and 0.84, successively as given in Table 3. The obtained $\alpha$ values show that, along the a-axis the compressibilities of $Ti_2AN$ (A = Si, Ge and Sn) compounds are bigger than that along the c-axis.

The estimated values of poisson's ratio ($\nu$), shear anisotropic factor ($A$), hardness ($H_v$) and linear compressibility coefficients ($\alpha$) for the $Ti_2SiN$ compound are quite consistent with previous theoretical studies [26,28].

Debye temperature ($\theta_D$) is a basic physical property. It is used to distinguish high and low temperature regions of solids. We have obtained the Debye temperature for $Ti_2AN$ (A = Si, Ge and Sn) compounds using the following equation [46],

$$\theta_D = \frac{h}{k_B}\left[\frac{3n}{4\pi V_A}\right]^{1/3} \nu_m \tag{9}$$

where $h$ is Plank's constant, $k_B$ Boltzmann's constant, $n$ number of atoms in the molecule, $V_a$ the atomic volume and $\nu_m$ averaged sound velocity. The average sound velocity in the polycrystalline material is given by Ref. [47],

$$\nu_m = \left[\frac{1}{3}\left(\frac{2}{\nu_t^3} + \frac{1}{\nu_l^3}\right)\right]^{-1/3} \tag{10}$$

where $\nu_l$ and $\nu_t$ are the longitudinal and the transverse sound velocity and are calculated in the following expressions of the bulk modulus ($B$) and shear modulus ($G$) [48],

$$\nu_l = \sqrt{\frac{3B + 4G}{3\rho}} \text{ and } \nu_t = \sqrt{\frac{G}{\rho}} \tag{11}$$

The calculated density ($\rho$ in g.cm$^{-3}$), the longitudinal, transverse and average sound velocity ($\nu_l$, $\nu_t$, $\nu_m$; in m.s$^{-1}$) and the Debye temperatures ($\theta_D$) for $Ti_2AN$ (A = Si, Ge and Sn) are presented in Table 4. The calculated density ($\rho$) values of $Ti_2AN$ (A = Si, Ge and Sn) compounds show the sequence of $\rho(Ti_2SiN) < \rho(Ti_2GeN) < \rho(Ti_2SnN)$ depending on the displacement of the $A$ atom. The density ($\rho$) according to this sequence is reduced by the increase of the ionic radius of $A$ atom, which is an expected result. The calculated Debye temperatures ($\theta_D$) of these three compounds indicate the ($Ti_2SiN$) > ($Ti_2GeN$) > ($Ti_2SnN$) order. These results show that the Debye temperature decreases when going from $Ti_2SiN$ to $Ti_2SnN$. Unluckily, there is no data available concerned about these properties in the literature for $Ti_2AN$ (A = Si, Ge and Sn).

### 3.3. Lattice dynamical and thermodynamic properties

Vibrations with low frequency corresponds to sound while

**Table 4**
The calculated density ($\rho$ in kg.m$^{-3}$), the longitudinal, transverse and average sound velocity ($\nu_l$, $\nu_t$, $\nu_m$; in m.s$^{-1}$) and the Debye temperatures ($\theta_D$) for $Ti_2AN$ (A = Si, Ge and Sn).

| Compounds | References | $\rho$ | $\nu_l$ (m/s) | $\nu_t$ (m/s) | $\nu_m$ (m/s) | $\theta_D$ (K) |
|---|---|---|---|---|---|---|
| $Ti_2SiN$ | Present | 4620 | 8436 | 4892 | 5429 | 716.4 |
| $Ti_2GeN$ | Present | 5840 | 6788 | 3689 | 4116 | 543.1 |
| $Ti_2SnN$ | Present | 6450 | 5979 | 3392 | 3772 | 479.5 |

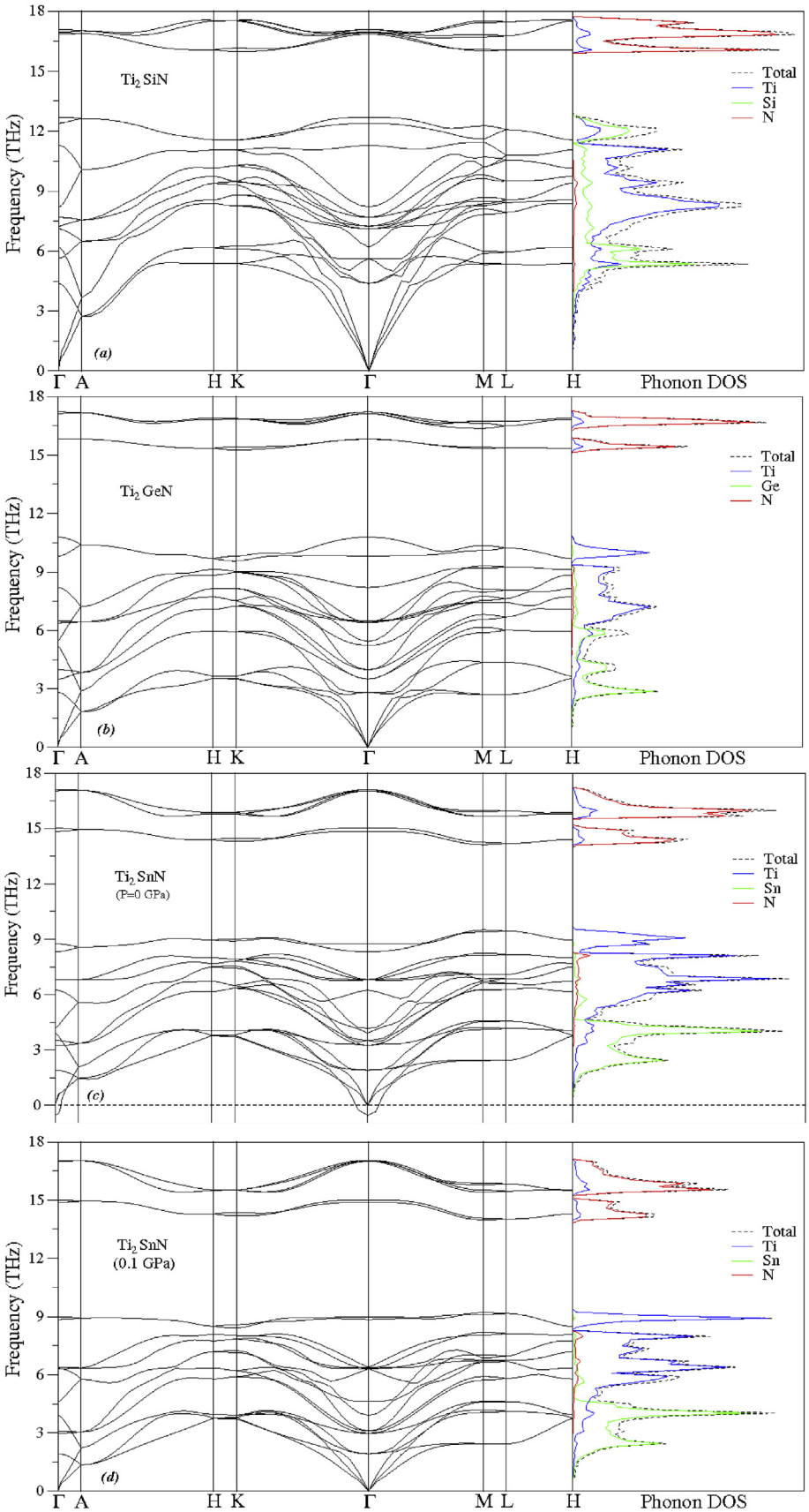


**Fig. 4.** The phonon dispersion curves, total and partial DOS of (a) $Ti_2SiN$, (b) $Ti_2GeN$, (c) $Ti_2SnN$ for P = 0 GPa and (d) $Ti_2SnN$ for P = 0.1 GPa.

vibrations with higher frequencies correspond to heat. At each frequency, quantum mechanics principles dictate that the vibrational energy must be a multiple of a basic amount of energy, called a quantum, that is proportional to the frequency. These basic levels of energy are called phonons in physics. Since there are 8 atoms in the primitive cell of MAX phase compounds in the hexagonal structure, there are 24 phonon branches in total, 3 of which are optical and 9 of which are optic. The coordinates of the special points of the BZ for hexagonal structure are Γ (0, 0, 0); A (0, 0, 1/2); K (2/3, 1/3, 0); H (2/3, 1/3, 1/2); M (1/2, 0, 0); L (1/2, 0, 1/2).

The calculated phonon dispersion curves and relevant partial and total density of states (DOS) in the absence of pressure for $Ti_2SiN$, $Ti_2GeN$ and $Ti_2SnN$ compounds are given in Fig. 4(a)-(b)-(c), respectively. The lack of negative frequency values in the calculated phonon dispersion curves indicate that $Ti_2SiN$ and $Ti_2GeN$ compounds are dynamically stable. On the other hand, it has been clearly seen that the calculated phonon dispersion curve at 0 GPa of $Ti_2SnN$ compound display softening behavior at Γ point as seen in Fig. 4 (c). Hence, $Ti_2SnN$ compound is dynamically unstable. The calculated phonon dispersion curve under the pressure 0.1 GPa for $Ti_2SnN$ is presented Fig. 4 (d). As seen in Fig. 4 (d), since there are no negative frequencies for $Ti_2SnN$, the material can be considered dynamically stable. This study is a reference, since there is no experimental or theoretical data available to compare these values.

As seen from the phonon dispersion curves of $Ti_2AN$ compounds, there is a gap between the optical-optical phonon modes. This gap is due to the difference in mass between Ti, A and N atoms. From the total phonon dispersion curves of $Ti_2AN$ (A = Si, Ge and Sn) compounds, these gap values were measured as 3.30, 4.48, 4.61 THz, respectively.

In Fig. 4 (a), for the $Ti_2SiN$ case, between 16 THz and 18 THz frequency range the majority of the phonon density of states (DOS) comes from N atom. Between 6 THz and 13.5 THz the most contribution to phonon DOS comes from Ti and Si atoms. On the other hand, between 4.5 THz and 6 THz range the majority oft he phonon DOS contribution comes from Si atom. However between 1.5 THz and 4.5 THz frequency range the most contribution comes from Ti atom.

In Fig. 4 (b), for the $Ti_2GeN$ case, between 15 THz and 18 THz the majority of the phonon DOS comes from N atom while the minority of the contribution comes from Ti atom. Between 6 THz and 11.6 THz frequency range the most contribution to phonon DOS comes from Ti atom. Between 1.5 THz and 6 THz frequency range the major contribution to phonon DOS comes from Ge atom.

In Fig. 4 (c), for the $Ti_2SnN$ case, between 14.8 THz and 18 THz, the most contribution to phonon DOS comes from N atom while the least contribution comes from Ti atom. Between 4.5 THz and 9 THz frequency range the major contribution to phonon DOS comes from Ti atom. However in the 0–4.5 THz frequency range the most contribution to phonon DOS comes from Sn atom.

For the $Ti_2AN$ (A = Si, Ge and Sn) compounds in the hexagonal structure, the vibration modes of thephonons at Γ point at $k = 0$ are classified by the irreducible notation of the point group $P6_3/mmc$ (No. 194). According to group theory, the symmetry of the modes of these point groups given as,

$$\Gamma(P6_3/mmc) = 3E_{1u} + 3A_{2u} + 2E_{2u} + 2E_{2g} + 2B_{2u} + 2B_{1g} + A_{1g} + E_{1g} \quad (12)$$

and the frequencies and symmetries of the modes of vibration calculated at Γ point of all compounds are cited in Table 5. At the Γ point, $E_{1u}$, $A_{2u}$ modes are infrared active, $A_{1g}$, $E_{1g}$ and $E_{2g}$ modes are raman active and $E_{2u}$, $B_{2u}$ and $B_{1g}$ modes are inactive. No comparison has been made since there is no study in the literature concerning the phonon frequencies of $Ti_2AN$ (A = Si, Ge and Sn) compounds.

**Table 5**
Calculated phonon frequencies (THz) at Γ point of $Ti_2AN$ (A = Si, Ge and Sn).

| Symmetry | $Ti_2SiN$ | $Ti_2GeN$ | $Ti_2SnN$ |
|---|---|---|---|
| $E_{2u}$ | 4.377 | 3.503 | 3.521 |
| $E_{2g}$ (R) | 5.627 | 2.818 | 1.909 |
| $B_{2u}$ | 6.188 | 5.232 | 4.178 |
| $E_{1u}$ (I) | 7.118 | 3.982 | 3.232 |
| $E_{1g}$ (R) | 7.252 | 6.481 | 6.784 |
| $E_{2g}$ (R) | 7.681 | 6.389 | 6.812 |
| $B_{1g}$ | 8.213 | 5.439 | 3.922 |
| $A_{1g}$ (R) | 11.288 | 9.815 | 8.314 |
| $A_{2u}$ (I) | 12.400 | 8.200 | 6.234 |
| $B_{1g}$ | 12.686 | 10.792 | 8.758 |
| $B_{2u}$ | 16.843 | 15.816 | 14.841 |
| $A_{2u}$ (I) | 16.917 | 15.823 | 15.020 |
| $E_{2u}$ | 16.956 | 17.126 | 17.042 |
| $E_{1u}$ (I) | 17.081 | 17.213 | 17.109 |

The obtained phonon dispersion results may be used to figure out temperature dependent thermodynamic properties, such as internal energy, entropy, free energy, and heat capacity. In the harmonic approach, the expressions of internal energy ($E$), free energy ($F$), entropy ($S$) and heat capacity ($C_v$) depending on the temperature with the help of phonons for each unit cell were calculated using the following equations [21].

$$E = \frac{1}{2} r \int_0^\infty g(w)(\hbar w)\cot h\left(\frac{\hbar w}{2k_B T}\right) dw \quad (13)$$

$$F = rk_B T \int_0^\infty g(w)\ln\left[2\sinh\frac{\hbar w}{2k_B T}\right] dw \quad (14)$$

$$S = rk_B \int_0^\infty g(w)\left\{\left(\frac{\hbar w}{2k_B T}\right)\left[\cot h\left(\frac{\hbar w}{2k_B T}\right) - 1\right] - \ln\left[1 - exp\left(\frac{-\hbar w}{k_B T}\right)\right]\right\} dw \quad (15)$$

$$C_v = rk_B \int_0^\infty g(w)\left(\frac{\hbar w}{2k_B T}\right)^2 \frac{exp\left(\frac{\hbar w}{k_B T}\right)}{\left[exp\left(\frac{\hbar w}{k_B T}\right) - 1\right]^2} dw \quad (16)$$

For the current study, thermodynamic properties such as specific heat, entropy, free energy and internal energy as a function of temperature are given in Fig. 5. In Fig. 5 (a), from the specific heat temperature relation for $Ti_2AN$ (A = Si, Ge and Sn), it is clearly seen that at $T \leq 200$ K specific heat increases rapidly while for $T > 200$ K the increase slows down. The obtained results show that specific heat values converge to Dulong-Petit limit [49] at high temperature. In Fig. 5 (b) entropy temperature relation is given for $Ti_2AN$ (A = Si, Ge and Sn). At low temperatures, the difference between $Ti_2SiN$, $Ti_2Ge$ and $Ti_2SnN$ is small. But as the temperature increases the difference becomes high. The entropy increases as a function of temperature for given alloys. Fig. 5 (c) is a sketch of the free energy as a function of temperature for $Ti_2AN$ (A = Si, Ge and Sn). It is clearly seen that free energy decreases while temperature increases.

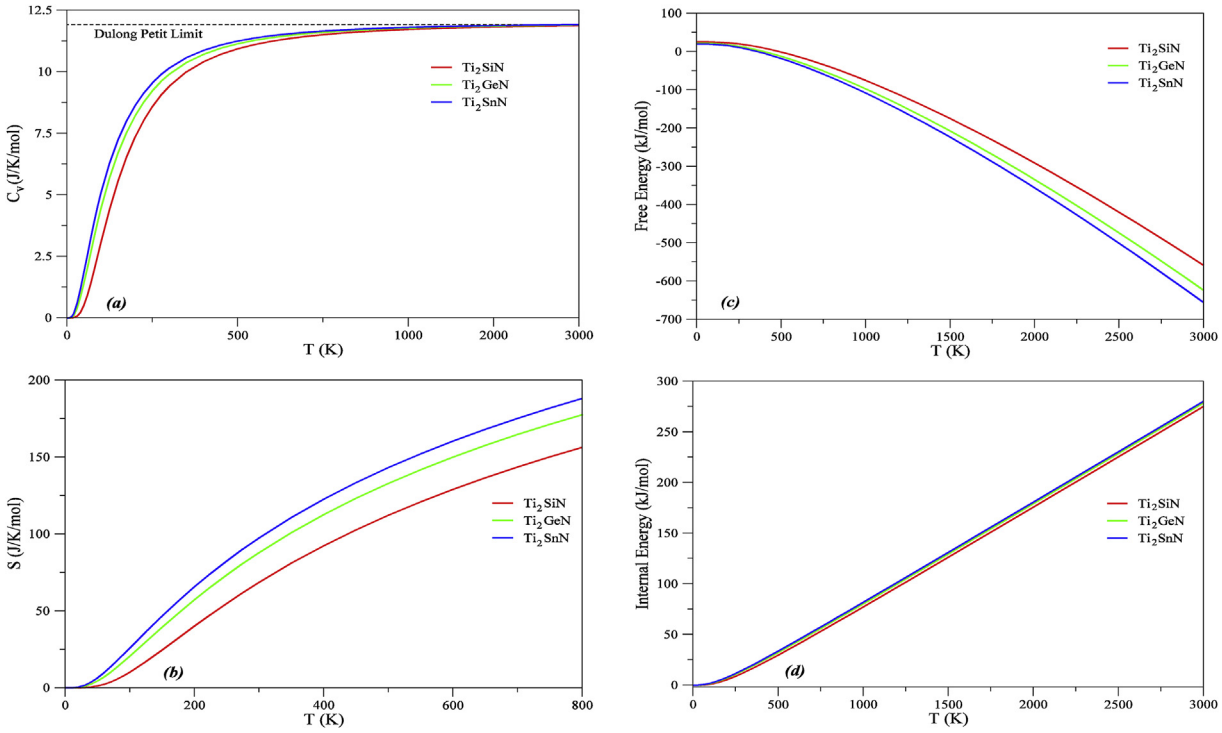


**Fig. 5.** (a) The specific heat capacity ($C_v$) at constant volume, (b) entropy ($S$), (c) helmholtz free energy ($F$) and (d) internal energy ($E$) versus temperature for $Ti_2AN$ (A = Si, Ge and Sn) compounds.

## 4. Conclusion

Density functional theory calculations within the framework of GGA have been carried out to have detailed information about the structural, electronic, mechanical, lattice dynamical and thermodynamic properties of $Ti_2AN$ (A = Si, Ge and Sn) compounds. Electronic band structure and corresponding total and density of states calculations revealed that these compounds are electrically conductive. Additionally, mechanical stability of these alloys has been analyzed through their elastic constants. It is observed that elastic constants obey the mechanical stability criteria. Ductility and brittleness of these compounds have been analyzed according to Pugh and it has been viewed that $Ti_2SiN$ is brittle while $Ti_2GeN$ and $Ti_2SnN$ are ductile. The obtained vickers hardness values showed that $Ti_2GeN$ has the smallest hardness and $Ti_2SiN$ has the highest hardness. Thermodynamic properties of these compounds have also been studied. It is observed that specific heat values converge to Dulong-Petit limit at high temperature. Obtained results for $Ti_2SiN$ are in good agreement with available theoretical data in literature. However, $Ti_2GeN$ and $Ti_2SnN$ results should be confirmed experimentally. Because this is the first theoretical study about these compounds. As far as we know this is the first comprehensive study about layered ternary nitrides $Ti_2AN$ (A = Si, Ge and Sn). Thus, results obtained in this study will be a good benchmark for future theoretical and experimental studies.

## References

[1] V.H. Nowotny, Strukturchemie einiger verbindungen der übergangsmetalle mit den elementen C, Si, Ge, Sn, Prog. Solid State Chem. 5 (1971) 27–70.
[2] H. Nowotny, P. Rogl, J.C. Schuster, Structural chemistry of complex carbides and related compounds, J. Solid State Chem. 44 (1982) 126–133.
[3] M.W. Barsoum, The $M_{N+1}AX_N$ phases: a new class of solids: thermodynamically stable nanolaminates, Prog. Solid State Chem. 28 (2000) 201–281.
[4] Z.J. Yang, J. Li, R.F. Linghu, X.L. Cheng, X.D. Yang, First-principle investigations on the structural dynamics of $Ti_2GaN$, J. Alloys Compd. 574 (2013) 573–579.
[5] X. He, Y. Bai, Y. Li, C. Zhu, M. Li, Ab initio calculations for properties of MAX phases $Ti_2InC$, $Zr_2InC$, and $Hf_2InC$, Solid State Commun. 149 (2009) 564–566.
[6] M.W. Barsoum, Physical properties of the MAX phases, in: K.H.J. Buschow (Ed.), Encyclopedia Mater. Sci. Technol., Elsevier, Amsterdam, 2006.
[7] Y.C. Zhou, Z.M. Sun, J.H. Sun, Y. Zhang, J. Zhou, Titanium Silicon Carbide: a Ceramic or a Metal?, 2000.
[8] P. Finkel, M.W. Barsoum, T. El-Raghy, Low temperature dependencies of the elastic properties of $Ti_4AlN_3$, $Ti_3Al_{1.1}C_{1.8}$, and $Ti_3SiC_2$, J. Appl. Phys. 87 (2000) 1701–1703.
[9] Z. Sun, Y. Zhou, M. Li, Oxidation behaviour of $Ti_3SiC_2$-based ceramic at 900–1300° C in air, Corrosion Sci. 43 (2001) 1095–1109.
[10] R. Radhakrishnan, J.J. Williams, M. Akinc, Synthesis and high-temperature stability of $Ti_3SiC_2$, J. Alloys Compd. 285 (1999) 85–88.
[11] Z.M. Sun, H. Hashimoto, Z.F. Zhang, S.L. Yang, S. Tada, Synthesis and characterization of a metallic ceramic Material–$Ti_3SiC_2$, Mater. Trans. 47 (2006) 170–174.
[12] T. El-Raghy, M.W. Barsoum, A. Zavaliangos, S.R. Kalidindi, Processing and mechanical properties of $Ti_3SiC_2$: II, effect of grain size and deformation temperature, J. Am. Ceram. Soc. 82 (1999) 2855–2860.
[13] Y. Zhou, Z. Sun, Microstructure and mechanism of damage tolerance for $Ti_3SiC_2$ bulk ceramics, Mater. Res. Innovat. 2 (1999) 360–363.
[14] M.W. Barsoum, H.I. Yoo, I.K. Polushina, V.Y. Rud, Y.V. Rud, T. El-Raghy, Electrical conductivity, thermopower, and hall effect of $Ti_3AlC_2$, $Ti_4AlN_3$, and $Ti_3SiC_2$, Phys. Rev. B 62 (2000) 10194.
[15] M.W. Barsoum, T. El-Raghy, C.J. Rawn, W.D. Porter, H. Wang, E.A. Payzant, C.R. Hubbard, Thermal properties of $Ti_3SiC_2$, J. Phys. Chem. Solid. 60 (1999) 429–439.
[16] W.Y. Ching, Y. Mo, S. Aryal, P. Rulis, Intrinsic mechanical properties of 20 MAX-phase compounds, J. Am. Ceram. Soc. 96 (2013) 2292–2297.
[17] A.S. Farle, C. Kwakernaak, S. van der Zwaag, W.G. Sloof, A conceptual study into the potential of $M_{n+1}AX_n$-phase ceramics for self-healing of crack damage, J. Eur. Ceram. Soc. 35 (2015) 37–45.
[18] W. Tian, P. Wang, G. Zhang, Y. Kan, Y. Li, D. Yan, Synthesis and thermal and electrical properties of bulk $Cr_2AlC$, Scripta Mater. 54 (2006) 841–846.
[19] J.M. Schneider, Z. Sun, R. Mertens, F. Uestel, R. Ahuja, Ab initio calculations and experimental determination of the structure of $Cr_2AlC$, Solid State Commun. 130 (2004) 445–449.
[20] C. Hu, C.-C. Lai, Q. Tao, J. Lu, J. Halim, L. Sun, J. Zhang, J. Yang, B. Anasori, J. Wang, Y. Sakka, L. Hultman, P. Eklund, J. Rosen, M.W. Barsoum, $Mo_2Ga_2C$: a new ternary nanolaminated carbide, Chem. Commun. 51 (2015) 6560–6563.
[21] G. Surucu, K. Colakoglu, E. Deligoz, N. Korozlu, First-principles study on the MAX phases $Ti_{n+1}GaN_n$ (n= 1, 2, and 3), J. Electron. Mater. 45 (2016) 4256–4264.
[22] G. Surucu, Investigation of structural, electronic, anisotropic elastic, and lattice dynamical properties of MAX phases borides: an Ab-initio study on

hypothetical $M_2AB$ (M= Ti, Zr, Hf; A= Al, Ga, In) compounds, Mater. Chem. Phys. 203 (2018) 106–117.
[23] Z. Lin, M. Zhuo, Y. Zhou, M. Li, J. Wang, Microstructures and theoretical bulk modulus of layered ternary tantalum aluminum carbides, J. Am. Ceram. Soc. 89 (2006) 3765–3769.
[24] J.P. Perdew, J.A. Chevary, S.H. Vosko, K.A. Jackson, M.R. Pederson, D.J. Singh, C. Fiolhais, Erratum: atoms, molecules, solids, and surfaces: applications of the generalized gradient approximation for exchange and correlation, Phys. Rev. B 48 (1993) 4978.
[25] P. Eklund, M. Beckers, U. Jansson, H. Högberg, L. Hultman, The $M_{n+1}AX_n$ phases: materials science and thin-film processing, Thin Solid Films 518 (2010) 1851–1878.
[26] Y.P. Gan, X.K. Qian, X.D. He, Y.X. Chen, S.N. Yun, Y. Zhou, Structural, elastic and electronic properties of a new ternary-layered $Ti_2SiN$, Phys. B Condens. Matter 406 (2011) 3847–3850.
[27] V.J. Keast, S. Harris, D.K. Smith, Prediction of the stability of the $M_{n+1}AX_n$ phases from first principles, Phys. Rev. B 80 (2009), 214113.
[28] H. Li, Z. Wang, G. Sun, P. Yu, W. Zhang, First-principles study on the structural, elastic and electronic properties of $Ti_2SiN$ under high pressure, Solid State Commun. 237 (2016) 24–27.
[29] G. Kresse, J. Hafner, Ab initio molecular dynamics for liquid metals, Phys. Rev. B 47 (1993) 558.
[30] G. Kresse, J. Furthmüller, Efficient iterative schemes for ab initio total-energy calculations using a plane-wave basis set, Phys. Rev. B 54 (1996) 11169.
[31] G. Kresse, D. Joubert, From ultrasoft pseudopotentials to the projector augmented-wave method, Phys. Rev. B 59 (1999) 1758.
[32] J.P. Perdew, K. Burke, M. Ernzerhof, Generalized gradient approximation made simple, Phys. Rev. Lett. 77 (1996) 3865.
[33] M. Methfessel, A.T. Paxton, High-precision sampling for Brillouin-zone integration in metals, Phys. Rev. B 40 (1989) 3616.
[34] H.J. Monkhorst, J.D. Pack, Special points for Brillouin-zone integrations, Phys. Rev. B 13 (1976) 5188.
[35] O.H. Nielsen, R.M. Martin, First-principles calculation of stress, Phys. Rev. Lett. 50 (1983) 697.
[36] K. Parlinski, Z.Q. Li, Y. Kawazoe, First-principles determination of the soft mode in cubic $ZrO_2$, Phys. Rev. Lett. 78 (1997) 4063.
[37] H. Baaziz, D. Guendouz, Z. Charifi, S. Akbudak, G. Uğur, Ş. Uğur, K. Boudiaf, Investigation of the structural, electronic, elastic and thermodynamic properties of curium monopnictides: an ab initio study, Int. J. Mod. Phys. B 31 (2017), 1750226.
[38] S. Akbudak, A.K. Kushwaha, G. Uğur, Ş. Uğur, H.Y. Ocak, Structural, electronic, elastic, optical and vibrational properties of $MAl_2O_4$ (M= Co and Mn) aluminate spinels, Ceram. Int. 44 (2018) 310–316.
[39] M. Born, K. Huang, Dynamical Theory of Crystal Lattices, Clarendon press, 1954.
[40] W. Voigt, Lehrbuch der Kristallphysik [The textbook of crystal physics], B.G. Teubner, Leipzig und Berlin, 1928.
[41] A. Reuss, Calculation of the liquid limit of mixed crystals on the basis of the plasticity condition for single crystals (Berechnung der Fliessgrenze von Mischkristallen auf Grund der Plastizitatsbedingung Fur Einkristalle), J. Appl. Math. Mech. 9 (1929) 49–58.
[42] R. Hill, The elastic behaviour of a crystalline aggregate, Proc. Phys. Soc. Sect. A. 65 (1952) 349–354.
[43] S.F. Pugh, XCII. Relations between the elastic moduli and the plastic properties of polycrystalline pure metals, Lond. Edinburgh Dublin Philos. Mag. J. Sci. 45 (1954) 823–843.
[44] Z. Sun, D. Music, R. Ahuja, J.M. Schneider, Theoretical investigation of the bonding and elastic properties of nanolayered ternary nitrides, Phys. Rev. B 71 (2005), 193402.
[45] X.Q. Chen, H. Niu, D. Li, Y. Li, Modeling hardness of polycrystalline materials and bulk metallic glasses, Intermetallics 19 (2011) 1275–1281.
[46] P. Wachter, M. Filzmoser, J. Rebizant, Electronic and elastic properties of the light actinide tellurides, Phys. B Condens. Matter 293 (2001) 199–223.
[47] O.L. Anderson, A simplified method for calculating the Debye temperature from elastic constants, J. Phys. Chem. Solid. 24 (1963) 909–917.
[48] O.L. Anderson, E. Schreiber, N. Soga, Elastic Constants and Their Measurements, 1973.
[49] P.L. Dulong, A.T. Petit, Recherches sur quelques points importans de la theorie de la Chaleur, 1819.